Published in final edited form as:
*Sci Transl Med*. 2013 February 20; 5(173): . doi:10.1126/scitranslmed.3005503.

# Safety and efficacy of an injectable extracellular matrix hydrogel for treating myocardial infarction

**S. B. Seif-Naraghi**[1,#], **J. M. Singelyn**[1,#], **M. A. Salvatore**[2], **K. G. Osborn**[1], **J. J. Wang**[1], **U. Sampat**[1], **O. L. Kwan**[1], **G. M. Strachan**[1], **J. Wong**[3], **P. J. Schup-Magoffin**[1], **R. L. Braden**[1], **K. Bartels**[1], **J. A. DeQuach**[2], **M. Preul**[4], **A. M. Kinsey**[2], **A. N. DeMaria**[1], **N. Dib**[1], and **K. L. Christman**[1,*]

[1]University of California, San Diego, La Jolla, CA USA, 92093

[2]Ventrix, Inc, San Diego, CA USA, 92109

[3]Biologics Delivery Systems, Irwindale, CA USA, 91706

[4]Barrow Neurological Institute, Phoenix, AZ USA, 85013

## Abstract

New therapies are needed to prevent heart failure after myocardial infarction (MI). As experimental treatment strategies for MI approach translation, safety and efficacy must be established in relevant animal models that mimic the clinical situation. We have developed an injectable hydrogel derived from porcine myocardial extracellular matrix (ECM) as a scaffold for cardiac repair post-MI. In this study, we establish the safety and efficacy of this injectable biomaterial in large-and small-animal studies that simulate the clinical setting. Infarcted pigs were treated with percutaneous transendocardial injections of the myocardial matrix hydrogel two weeks post-MI and evaluated after three months. Echocardiography indicated improvement in cardiac function, ventricular volumes, and global wall motion scores. Furthermore, a significantly larger zone of cardiac muscle was found at the endocardium in matrix-injected pigs compared to controls. In rats, we establish the safety of this biomaterial and explore the host response via direct injection into the left ventricular lumen and in an inflammation study, both of which support the biocompatibility of this material. Hemocompatibility studies with human blood indicate that exposure to the material at relevant concentrations does not affect clotting times or platelet activation. This work therefore provides a strong platform to move forward in clinical studies with this cardiac-specific biomaterial that can be delivered by catheter.

[*]Corresponding author: christman@eng.ucsd.edu.
[#]Contributed equally.

**Supplemental Materials**
Materials and Methods
Table S1. Quantitative averages of Holter monitoring data.
Table S2. Qualitative comparison of Holter monitoring data.
Fig S1. Histological assessment of peripheral organs in porcine study.
Fig. S2. Histological assessment of lungs in small animal safety study.

**Author contributions**: KLC, AMK, and ND obtained the funding. KLC, AND, and ND designed the porcine experiments. SBS-N designed and executed all small animal work and wrote the manuscript. JMS, MAS, KB, KGO, AND, and ND performed the porcine studies. The acquisition and/or analysis of data was handled by SBS-N, MAS, KGO, JW, JAD, US, OLK, GMS, JW, AND, and ND. Drafting and/or revising the manuscript for critical content was executed between by KLC, SBS-N, JAD, JMS, KO, and MAS. Administrative, technical, or supervisory tasks were handled by KLC, KB, ND, AND, and MP.

**Competing interests**: KLC, AMK, AND, ND, JAD, and MAS are equity holders; KLC and AMK are board members; and AND and ND are on the scientific advisory board of Ventrix, Inc. JMS, JAD, KLC, and AMK are inventors on patent applications (US20120156250, US20110189140) associated with this work and owned by the University of California, San Diego.

**Materials and data availability**: Full pathology report of animal tissues is available upon request..

## INTRODUCTION

As medical management and surgical tools advance, a growing number of patients survive heart attacks. Unfortunately, many then develop heart failure (HF), for which the five-year survival rate is only 50% (1). Thus, there is a pressing clinical need for new therapies to prevent progression of the negative left ventricular remodeling that follows myocardial infarction (MI) and leads to HF. During MI, a blockage in a coronary artery causes cell death followed by degradation of the associated extracellular matrix (ECM) and an acute inflammatory response. Owing to the limited regenerative capacity of the myocardium, the injury is resolved with formation of a dense collagenous scar. This scar cannot contribute to the pumping function of the heart and over time the remote myocardium hypertrophies to compensate, the infarct wall continues to thin, the ventricle dilates, and ultimately the heart fails. The only successful treatments for end-stage HF are total heart transplantation and left ventricular (LV) assist devices; however, the former is limited by a severe lack of donor organs, the latter relies on chronic use of an external device, and both require invasive, inherently risky surgical procedures.

Experimental approaches to mitigate negative remodeling and prevent HF include LV restraints, cardiac patches, *in situ*-gelling biomaterials, and cell transplantation. Interest in LV restraints has waned considerably over the past 5 years as focus has turned toward more targeted, biodegradable strategies. Cellular cardiomyoplasty has been used experimentally in the clinic with some success, but continues to be limited by poor cell survival and retention post-implantation. Scaffold biomaterials vary widely (2–4), and most work has shown that these materials can provide maintenance or improvement in functional parameters in small animals and some large-animal models either alone, or with cells or growth factors. However, the majority of these approaches will not transition to minimally invasive delivery in the clinic: patches require a thorocotomy for epicardial placement and most existing injectable biomaterials are not compatible with cardiac catheter procedures, which require the material to be in the catheter up to 1 hour (5, 6).

ECM-based materials have emerged as a promising class of naturally derived biomaterial scaffolds. Given the tissue specificity of the ECM, it follows that the most appropriate scaffold to replace the damaged ECM after a MI would be derived from myocardial tissue. We previously developed an injectable ECM hydrogel derived from decellularized porcine myocardial tissue (7), which self-assembles into a porous and fibrous scaffold upon injection into tissue, and recently demonstrated that injecting this ECM hydrogel post-MI in a rodent model mitigated LV remodeling and preserved ejection fraction (8). However, to translate this material to the clinic, we needed to address the biocompatibility and safety of this ECM-derived material and investigate efficacy in a clinically relevant large-animal model. Biocompatibility of injectable extracellular matrix hydrogels for this application has been indirectly supported in the literature (7, 9) and the immune response to decellularized ECM grafts placed subcutaneously has been explored (10–12), but little work has been done to explore the site-specific tissue response to these materials over an extended time course or to understand the hemocompatibility and thrombo-embolic potential of these materials. Moreover, large-animal studies are crucial to explore the effectiveness of an ECM-derived hydrogel for tissue repair. In this study, we show that the myocardial matrix hydrogel can be used to prevent negative remodeling and HF in a clinically relevant porcine MI model and further establish the safety and biocompatibility of the material in rodent studies.

# RESULTS

## Myocardial matrix improves cardiac function and mitigates negative remodeling

A porcine model was used to assess the efficacy of myocardial matrix injections for treatment after MI. Two weeks post-MI, transendocardial injections of a myocardial ECM-derived hydrogel (myocardial matrix) and saline were delivered to the ischemic region using a catheter traditionally used for cellular cardiomyoplasty procedures. Two pigs received no injections owing to limiting factors during the procedure. Echocardiography data showed improvements in cardiac functional parameters in the matrix-injected animals and a worsening of function in the control animals (Table 1). Parameters measured included ejection fraction (EF), which is a measure of cardiac function, and LV end diastolic volume (EDV) and end systolic volume (ESV). There was no statistical difference between the two groups prior to MI or at two weeks post-MI (pre-injection) ($P > 0.05$, Student's t-test). However, at the time of euthanasia (3 months post-injection), EF of the matrix group was significantly greater, and EDV and ESV were significantly smaller than those of the control animals (Table 1).

Figure 1A displays individual animal data at pre-MI, pre-injection (2 weeks post-MI), and pre-euthanasia (3 months post-injection). One saline-injected animal was euthanized 2 months post-injection. Injection of the myocardial matrix resulted in an improvement in EF in 5 out of 6 animals, whereas 3 out of 4 control animals worsened (Fig. 1A). EDV was decreased in 50% of the matrix-injected animals, whereas it increased in 75% of the control animals (Fig. 1A). Lastly, the ESV improved with myocardial matrix injection in 4 out of 6 animals, whereas every control animal had increased ESV (Fig. 1A).

As seen in control data in Fig. 1A, one animal (in green) had a larger ventricle prior to MI compared to other animals in the study; this contributes to the large variability in the data presented in Table 1 and makes comparisons between the two groups based solely on averages more difficult to compare. We therefore compared absolute changes in functional parameters between groups (Fig. 1B). For changes from euthanasia to pre-MI baseline values, the decline in EF and increase in EDV and ESV was significantly smaller with myocardial matrix treatment compared to controls (Fig. 1B). The change from euthanasia to pre-injection (2 weeks post-MI) for ESV of the matrix group was significantly smaller compared to controls, with similar trends towards improvement in EF and EDV (Fig. 1B).

Global wall motion index (GWMI) scores corroborated these functional data. Wall motion is scored as normal (1), hypokinetic (2), akinetic (3), or dyskinetic (4). Treated animals regained a more normal GWMI over the course of the study, whereas control animals continued to worsen (Fig. 1C). Regional dysfunction, as implied by an increased wall motion score, was similar in both groups at each time point until after treatment, at the final echo, at which point the control animals had a significantly larger average GWMI than the treated group. These data support the potential for the myocardial matrix to mitigate the negative LV remodeling observed post-MI, specifically by improving systolic function and contractility.

In addition to echocardiographic measurements, electromechanical NOGA® data were collected pre-injection (2 weeks post-MI) and pre-euthanasia (3 months after injection) from all 6 matrix-injected animals and 2 of the control animals. Two control animals did not receive NOGA® mapping owing to a clot in the LV that prevented mapping in one non-injected animal and the death of the second saline animal at 2 months. Unipolar and linear length shortening (LLS) methods were both used to calculate the change in infarct size over the course of the experiment. Representative unipolar map changes are illustrated for a control animal's heart and a matrix-injected heart in Fig. 2A, where the red area indicates

decreased conduction and is indicative of the infarct area. By the unipolar method, infarct size in matrix-injected hearts had a average fractional increase of 2.1, from 6.5 ± 2.9 $cm^2$ to 9.3 ± 2.5 $cm^2$, whereas infarct size in control animals had a average fractional increase of 11.0, from 2.8 ± 2.4 $cm^2$ to 19.1 ± 11.9 $cm^2$ (mean +/− SEM) (Fig. 2B). By the LLS method, infarct size in matrix-injected hearts had a fractional decrease of 0.3, from 6.5 ± 3.1 $cm^2$ to 4.9 ± 3.2 $cm^2$, and infarct size in control animals had a fractional increase 17.5, from 9.2 ± 8.7 $cm^2$ to 16.0 ± 2.2 $cm^2$ (Fig. 2C).

### Myocardial matrix enhances cardiac muscle and reduces infarct fibrosis

At the end of the study, hearts were removed and tissue sections at the mid-infarct point were examined. The infarcted areas from the two groups showed distinct differences in endocardium morphology (Fig. 3). Masson's trichome staining revealed that all matrix-injected hearts had a distinct band of muscle along the endocardium (Fig. 3A). The non-injected control animals had an endocardium that appeared as a thin layer with endothelium, with a loose fibrillar layer beneath the endothelium (Fig. 3B). In saline-injected control animals, the endocardium was moderately thickened and showed minimal muscle formation (Fig. 3C). The red-stained zone was verified to be cardiomyocytes by staining adjacent slides with anti-cardiac Troponin-T (Fig. 3D). The area of this endocardial muscle layer as a proportion of the total infarct size was quantified and found to be significantly larger in the matrix-injected animals compared to control animals (Fig. 3E). We also quantified the percent fibrosis in the infarct and found that matrix injection significantly reduced the percentage of collagen within the infarct compared to controls (Fig. 3F). There were also foci of neovascularization present in the area below the endocardium of all matrix-injected hearts (Fig. 3G). None of the control hearts showed similar foci of neovascularization (Fig. 3H).

### Myocardial matrix does not adversely affect peripheral tissues, cardiac rhythm or blood chemistry in treated pigs

Tissue samples were taken from peripheral organs (kidneys, brain, spleen, liver, lungs, and skeletal muscle) of the pigs and examined by a pathologist blinded to the study groups. There were no substantial differences between the two groups. The differences that were observed were interpreted as incidental lesions that were not associated with the experimental treatments. These included mild liver lesions such as mild centrilobular congestion in one matrix-injected animal and mild multifocal mononuclear cells (lymphocytes with or without other lymphoid cells) in 3 matrix animals. One common lesion identified as a post-mortem artifact was splenic red pulp congestion in all animals except two of the controls (fig. S1).

ECG data from matrix injection showed no abnormalities in rhythm or waveform morphology. No matrix injection-related effect on the heart rate or RR, PR, QRS, QT, or QTc intervals was found based on comparison of pre-and post-injection values and control values (table S1). In the Holter data, infrequent short periods of non-sustained ventricular tachycardia were found in 3 of the matrix-injected animals. In 2 of the 3 animals tachycardia occurred prior to injection of myocardial matrix; in a third animal, one period of 5 pre-ventricular contractions (PVCs) were observed one week post injection (table S2). Based on comparison of pre-and post-injection mean ECG recordings to the control animal ECG recordings, all the ECGs were considered normal for Yucatan pigs.

Clinical laboratory assays for the matrix-injected animals were also considered normal at each time point (pre-MI, pre-injection, and pre-euthanasia), with the exception of a low fibrinogen reading (55 mg/dl) at the time of euthanasia for one animal.

### Myocardial matrix is biocompatible and biodegradable

We also examined the safety and biocompatibility of the myocardial matrix using rodents and human blood samples. Healthy rats received intramyocardial injections of decellularized porcine myocardial matrix (PMM), saline, or a non-decellularized porcine myocardial matrix (NDM) and then euthanized for histological evaluation after 1, 3, 7, 14, 28, 56, or 112 days (n = 3 per timepoint per group). The PMM was identifiable in tissue sections on days 1, 3, and 7. In 1 of 2 hearts evaluated, PMM was still present at 14 days, but was completely degraded in all 3 hearts by 28 days (Fig. 4). On average, lesion areas in NDM-injected animals were 40% larger than lesion area in PMM-injected animals (9980 +/− 1842 $\mu m^2$ vs. 7125 +/− 1126 $\mu m^2$), and 45% larger than saline-injected animals (6887 +/− 1441 $\mu m^2$) (mean +/− SEM). Initially, the inflammation in PPM-injected animals was overall greater than saline-injected animals; however, both were resolved at 56 and 112 days.

Cellularity of the injected areas was assessed using a scoring system where cell infiltration was either absent (0), minimal (1), mild (2), moderate (3), or marked (4). These scores did not take the size of the lesion into consideration, but rather the degree to which the cell type was represented in the cell infiltrate. Thus, when two groups have similar scores, it is a reflection that they have similar composition of infiltrating cells, not that the overall degree of inflammation is the same. NDM-injected animals had lesions that were higher in cellularity and area, over the entire course of the study. In all groups, there was an acute inflammatory response characterized by an early peak in infiltrating polymorphonuclear cells (PMNs) that decreased over time (Fig. 5A). Lymphocytes were a dominant cell type in the NDM group, but appeared to a lesser degree in the saline and PMM groups at all time points (Fig. 5B). Large mononuclear cells (macrophages) were present during inflammation in all groups, although they were more dominant in the NDM group at early timepoints compared to the saline and PMM groups (Fig. 5C). Spindle cells (fibroblasts, myofibroblasts, and cardiomyocytes) became dominant cell types in the saline-and PMM-injected groups after two weeks (Fig. 5D), indicating a reparative response. Importantly, signs of chronic inflammation, including multinucleated giant cells were only observed in the NDM group (Fig. 5E), and not in the PMM-or saline-injected groups (Fig. 4 and Fig. 5E). Given the semi-quantitative nature of these data, statistical analysis was not performed. These cell infiltration data demonstrate the biocompatible nature of the myocardial matrix when appropriately processed (decellularized) to remove the cellular content.

### Matrix injection does not cause embolization or ischemia

The second approach to verifying the safety of this treatment was via direct injection into the LV lumen in rats. Leakage can occur with transendocardial injection, so it is important to understand the hemocompatibility and thrombo-embolic potential of the material in the event that the material enters systemic circulation. Rats that received direct injections of myocardial matrix (n = 4) or saline (n = 2) into the lumen of the LV were revived and observed for 6 hours. All rats recovered normally and showed no signs of stress or discomfort prior to euthanasia. Histological examination of kidneys, heart, brain, spleen, liver, and skeletal muscle found no signs of acute ischemia or thrombus, and the degree of edema, hemorrhage, and inflammation was minimal and not different between groups. There was a moderate degree of edema and inflammation in the lungs, but it was similar between saline-and matrix-injected animals and attributed to trauma associated with the surgery (fig. S2).

### Human blood tests show hemocompatibility of myocardial matrix

We examined the interaction between the injected matrix and human blood with respect to clotting times and platelet activation. Myocardial matrix was evaluated at different concentrations in blood. The “standard” concentration reflected a conservative estimate of

the amount of matrix that would be injected into the bloodstream if the needle disengaged from the endocardium. Addition of the myocardial matrix to human plasma had no effect on activated partial thromboplastin time (APTT) or prothrombin time (PT) (Table 2). At both the standard concentration (volume ratio 1:10,000) and a higher concentration (1:2500), APTT and PT remained within reference ranges (Table 2).

Additionally, exposure of platelet-rich-plasma (PRP) to myocardial matrix at standard estimates did not cause platelet activation, as indicated by a constant turbidity (Fig.6). At a "high" concentration (2.5 times the standard concentration, or volume ratio 1:4,000), minimal platelet activation was observed, as indicated by the dip in turbidity after 3 minutes (Fig. 7B). The addition of agonists after 5–10 minutes resulted in normal platelet activation, as indicated by the sharp decrease in turbidity (Fig. 6, A and B). After four hours, the quality of the sample was verified by adding agonists directly to time-matched control PRP samples and observing normal activation curves (Fig. 6C).

## Discussion

Confirming the success of previous small-animal work (8), this study demonstrates efficacy and feasibility in a clinically relevant porcine MI model, where both the pathophysiology and the administration mimic what would be observed and performed in humans, as well as addresses important remaining safety issues. In the present study, we demonstrate the potential for an injectable myocardial matrix hydrogel to improve cardiac function, prevent negative LV remodeling, and increase cardiac muscle after MI in a porcine model.

Decellularized matrix materials have been used as "nature's platform" for a variety of tissue regeneration applications, and injectable hydrogels derived from small intestinal submucosa (SIS) and pericardium have both been investigated for cardiac repair in rodent models (13, 14). Because the ECM is specific to each tissue, the myocardial ECM can potentially provide appropriate tissue-specific cues for infiltrating cells. *In vitro*, biochemical cues from the myocardial matrix have been shown to promote maturation of human embryonic stem cells (15), and cardiac differentiation and survival of cardiac progenitor cells (16). It is known that there are more cardiac progenitor cells in failing hearts (17), so by mitigating the harsh infarct milieu, the injected matrix may also provide a more appropriate environment as well as a physical scaffold for circulating stem cells to encourage repair and regeneration (8). In the rat MI model, we observed larger clusters of cardiomyocytes in the infarct area at 1 week post-injection, which we postulated was a result of improved cardiomyocyte survival (8). In the porcine model, we observed a significantly larger area of cardiac muscle accompanied by areas of neovascularization at the endocardium 3 months post-injection in treated animals compared to control animals. This may be a combination of preserved cardiomyocytes and newly formed cardiomyocytes, as we previously observed proliferative cardiac Troponin-$T^+$ cells and c-$kit^+$ cells within the matrix in the rat MI (8). This also suggests that the myocardial matrix contributes to improvements in contractility by increasing a layer of muscle at the endocardium, which is where the biomaterial is delivered. Injection of other materials, such as peptide nanofibers, have also shown newly formed cardiomyocyte-like cells, but co-delivery with a growth factor (VEGF) was required (18). In this study, the material alone increased cardiac muscle and improved contractility.

There are several important design considerations that must be met for injectable biomaterials to be useful and relevant treatments for MI. One that is crucial to clinical translation is the delivery method. Although several injectable biomaterials have shown promising results in small animals, few have been translated to percutaneous delivery in large animals. To date, the only other material to be delivered percutaneously in a large animal MI model is alginate (19). Leor *et al* demonstrated success with intracoronary

infusion of alginate in pre-clinical work in swine (19), which led to delivery in a small Phase I/II study in acute MI patients (ClinicalTrials.gov identifier NCT00557531), and an ongoing Phase II clinical trial (NCT01226563). The myocardial matrix is the second material to be delivered percutaneously in a large MI model and the first material to be delivered via a transendocardial approach. Transendocardial delivery is considered by many to be the preferred method of catheter delivery (20–22). This method allows for guided, direct intramyocardial delivery, which increases biomaterial retention and does not require access to the coronary vessels, reducing the risk of embolization. Additionally, the coronary access required for intracoronary delivery is often compromised in the target patient population. Here, we chose to inject 2 weeks post-MI, the same time point we previously used rats (8). Injection is generally considered risky in the clinic in the first week post-MI because of the potential for ventricular rupture due the unstable ventricular wall caused by matrix metalloproteinase (MMP) upregulation. Moreover, injection immediately post-MI would likely cause premature degradation of our ECM-derived scaffold at the same time the native ECM is being degraded.

Echocardiographic GWMI, which is a measure of regional function, has been shown to be a significant predictor of cardiovascular death after acute MI and has independent prognostic value when added to a model that includes EF and other baseline clinical values (23, 24). The reduction in this parameter in matrix-injected animals implies improvement in regional function and contractility. In addition to the improved GWMI and EF in the matrix-injected animals, LV volumes also demonstrated a positive change. In HF patients, increases in ESV indicate a decline in contractility. This pattern is observed in the controls, where the LV ESV continues to increase post-MI. The matrix group, however, had on average a decreased ESV compared to the controls. This implies that the myocardial matrix may provide a method for preventing the negative remodeling of the ventricle that precedes HF, and improving systolic function, potentially through the increase in cardiomyocytes observed at the endocardium. We found improvements in global and regional cardiac function and LV volumes, whereas alginate, the only other material to be delivered percutaneously in a large MI animal model, significantly changed LV geometry, but not fractional shortening (19). Other hydrogels alone, such as fibrin-alginate (25), hyaluronic acid (26), and peptide nanofibers (27), which have been delivered in large animals using direct injection (non-catheter-based), have likewise not improved EF. Our data also supported safety with respect to the effect on cardiac electrophysiology. Ectopic beats and QRS changes were seen as a result of the infarction procedure in both the matrix-injected and control animals; no additional abnormalities occurred as a result of the injection.

Evaluation of the local tissue response to decellularized ECM biomaterials injected in the myocardium has not been described previously. Performing this study in rats allowed us to evaluate the material in a xenogeneic model. The increased presence of spindle cells, which include fibroblasts, myofibroblasts, and cardiomyocytes, observed in the matrix group supports a reparative remodeling response. Interestingly, this is corroborated by the cardiomyocyte populations identified in the infarcts of matrix-injected pigs. Signs of chronic inflammation – persistent lymphocyte presence and the appearance of multinucleated giant cells – were only observed in the non-decellularized control. This implies the response to cellular debris is both more severe and may be associated with rejection or a foreign body response, rather than the remodeling response seen with decellularized matrix materials, which is consistent with previous work with decellularized grafts (28). Here we show degradation of the matrix between 14 and 28 days and an appropriate inflammatory response that may promote remodeling. In this study, we used only porcine-derived matrix as that is the most viable source as a clinical product because human tissue has greater variability and collection of healthy human hearts is limited; many porcine derived-ECMs are also already approved by the FDA (29).

An important criterion for translation is lack of thrombogenicity and in this work we demonstrate myocardial matrix to be non-thrombogenic upon direct injection into the LV lumen. The lack of post-procedural distress in rats indicated no major event and we found no difference in tissue morphology in peripheral organs in both matrix-and saline-injected animals. These findings are supported by a similar lack of significant findings in the tissue analyzed from the pigs in the large animal study. When injected directly into the LV lumen, myocardial matrix is immediately diluted upon injection into the bloodstream, and therefore likely does not have a chance to self-assemble and is quickly degraded and cleared. In contrast, a synthetic or naturally-derived biomaterial that gels very quickly or causes protein aggregation could cause detrimental clot formation in the LV or peripheral vasculature (30).

In addition to thrombogenicity of an injected material, it is also essential to understand potential interactions between the matrix and the host blood. Clotting times are an important clinical parameter, especially for patients under medical management for cardiovascular diseases. Herein, the matrix was shown to be hemocompatible in human blood, as there was no change in clotting times with the addition of the material and no platelet activation with the addition of the standard material concentration. The slight activation observed with the high concentration of myocardial matrix is expected, as collagen is a significant component of ECM hydrogels (8) and an agonist; the observed level of activation is, however, not considered clinically relevant.

Although the data generated support the efficacy and safety of this biomaterial therapy, there are limitations to this work. For example, a conventional pharmacologic regimen was not employed, such as ACE inhibitors or beta blockers. Additionally, the pig numbers were small, with the 4 controls in the porcine functional study combining both saline injection and no injection. Although this study would have been strengthened by more saline-injected animals, previous work with this porcine MI model has shown that cell growth medium-injected control animals similarly declined post-injection (31), which corroborates our control data. Additionally, similar animal numbers per group have been used in large animal pre-clinical MI studies that have been deemed sufficient to initiate clinical trials (19, 31, 32). These previous studies examined cardiac function out to two months after MI, while we examined functional parameters out to 3 months post-injection, which is well beyond the material degradation time of 2–3 weeks. Despite a low number of control animals, the functional changes seen in the cardiac functional data within the matrix-treated group are promising – particularly the improved ESV, which is considered to be the best clinical predictor of survival post-MI (33, 34), as well as improved regional contractility as indicated by the improved GWMI.

In summary, we have established the safety and efficacy of an injectable myocardial matrix biomaterial in preclinical large-and small-animal studies. This work, taken in conjunction with previous small animal studies with the same material (8), provides support for the advancement of this technology from preclinical studies to a first-in-human study.

## Materials and Methods

### Preparation of injectable ECM hydrogels

Ventricular porcine myocardium was decellularized using sodium dodecyl sulfate (SDS) and processed into an injectable ECM hydrogel via lyophilization and partial pepsin digestion (7, 8). Decellularization and ECM preparation protocols can be found in Supplementary Methods. Non-decellularized porcine myocardial matrix (NDM) was prepared according to the same protocols (Supplementary Methods) except that the fresh tissue was frozen, lyophilized, milled, and digested without decellularization.

### Porcine procedures

All experiments were performed in accordance with the guidelines published by the Institutional Animal Care and Use Committee at the University of California, San Diego, and the American Association for Accreditation of Laboratory Animal Care.

MI was induced in mature Yucatan mini-pigs (45 – 50 kg) via the percutaneous coil embolism infarct model, as developed and validated by Dib et al (31, 35). Prior to MI, a 12-lead ECG and echocardiogram were obtained to ensure the animal was healthy. On each animal, a sheath was inserted into either the right or left femoral artery, allowing catheter access to the artery and retrograde access to the LV through the aorta. The anesthesia protocol is detailed in Supplementary Methods.

MI was induced by the deployment of 1–2 complex helical fibered platinum coils (Boston Scientific) within the left anterior descending (LAD) coronary artery. If the first coil did not occlude the artery, a second coil was deployed. Following each coil deployment, the ECG was monitored for changes, and ST elevation was considered to be indicative of occlusion. Post-MI angiograms were performed to confirm arterial occlusion. Animals were carefully monitored until fully recovered from anesthesia. Resuscitation via electrical cardioversion (360 J) was administered if the animal experienced sustained ventricular tachycardia.

Approximately two weeks post-MI (12 – 14 days), myocardial matrix or saline was injected into the infarct area via percutaneous transendocardial delivery. Anesthesia was administered as in the MI procedure, described in Supplementary Methods. Arterial access was gained on either the left or right femoral artery, and a NOGA map was created of the endocardial wall to identify the infarcted region. A Biosense Webster Type B injection catheter was used for injections, and its needle length in the straight and curved position was adjusted to be 3.5 mm straight. The injection catheter was flushed with myocardial matrix prior to insertion. The NOGA map was used to guide injections throughout the infarct, and border zone. Fresh material was pulled up into a new 1 mL syringe for each set of injections, to allow for 14–15 injections of 0.25 mL for a total of 3.5 – 3.75 mL in each animal. Animals were recovered and euthanized 3 months after injection. NOGA mapping was repeated prior to euthanasia. The infarct area was determined as the area below 6.9 mV and 6% on the unipolar and LLS maps, respectively (36). ECGs, Holter monitoring, echocardiography, and angiography methods are described in Supplementary Methods. Animals were fasted overnight prior to each surgical procedure (MI, injection, euthanasia), and blood draws were performed from femoral access under anesthesia.

Of the 14 infarcted pigs, two died within 24 hours of the MI procedure, 6 received myocardial matrix injections, 2 received saline injections, and 2 received no injections owing to limiting factors during the procedure (thrombus in the LV that prevented visualization of the endocardial border and complications in the placement of the catheter sheath that prevented use of the injection catheter). One pig in the saline-injected group was euthanized after two months because of suffering caused by the infarct; data from this animal is included. One pig in the saline-injected group was identified as having hypertrophic cardiomyopathy upon euthanasia and examination of the pre-MI echocardiogram; data from this animal was excluded. The first pig in the myocardial matrix-injected group died 24 hours post-injection. This animal was the only surviving pig to require multiple electrical cardioversions as a result of sustained ventricular tachycardia during the MI procedure, and had the lowest EF of all animals pre-injection. The only notable finding upon necropsy of this pig was multifocal thromboemboli and associated parenchymal changes (congestion, atelectasis), plus pulmonary venule and small vein luminal neutrophilia in the lungs, which is likely associated with the induced MI. Although

it cannot be conclusively ruled out, matrix injection was unlikely to result in this pathology given that any leakage from injections would go into the arterial blood stream.

Animals from which data were collected for this study include 6 myocardial matrixinjected animals and 4 control animals (2 saline-injected, 2 not injected). Unless otherwise specified, all “control group” data presented in this study is from these 4 animals.

### Small animal surgery protocol

Female Sprague Dawley rats (225–250 g) were anesthetized with 5% isoflurane and then maintained at 2.5% isoflurane for the remainder the procedure. Using aseptic technique, injections into the left ventricular free wall were performed, following a well-described protocol (37). Briefly, animals were placed in supine position and an incision was made from the xyphoid process along the abdomen. A small incision was made in the diaphragm to access the apex of the heart. Samples of NDM, PMM, or saline (75 μL) were drawn up into a syringe and injected into the LV free wall through a 30-gauge needle. On days 1, 3, 7, 14, 28, 56, and 112 post-injection, three animals per group were euthanized.

For the direct injection safety study, 75 μL of PMM or saline was injected directly into the lumen of the LV. The animals were revived and maintained for six hours after the procedure and before euthanasia. After an i.p. injection of 400 uL of FatalPlus (Vortech Pharmaceuticals), the animals were perfused with PBS followed by 10% buffered formalin. After perfusion, the following organs were removed for histological analysis: spleen, brain, lung, heart, kidneys, liver, and skeletal muscle.

### Histological analyses

For the direct lumen injected rats and all pigs, tissue was fixed, paraffin-embedded, and then sectioned. For the biocompatibility study, hearts were fresh frozen and cryosectioned. All tissues were analyzed in a blinded fashion by experienced pathologists (K.G.O and G.J. Kolaja, Balboa BioConsulting, Inc).

H&E-stained sections from direct lumen injected rats were examined for evidence of acute ischemia, edema, hemorrhage, and inflammation in each organ. In the biocompatibility study, 3 H&E-stained slides representing the largest portion of the affected region from each rat heart were evaluated with a single score per animal (absent = 0, minimal = 1, mild = 2, moderate = 3, marked = 4) with respect to infiltrating multinucleated giant cells, PMNs, lymphocytes, large mononuclear cells, and spindle cells.

For the pig hearts, sections (one H&E, one Masson’s trichrome) representing the mid-infarct were analyzed. Additionally, immunohistochemistry was used to identify cardiac-specific Troponin-T-positive cells (Pierce, 1 μg/mL); an HRP-conjugated secondary antibody and metal-enhanced diaminobenzidine (DAB) substrate (Thermo Scientific Pierce) were used for visualization. Slides were counterstained with hematoxylin. AxioVision software was used to outline the infarct area and an automated program was written to count blue pixels (positive for collagen) within that region in trichrome images. The red-stained tissue near the endocardium was outlined and the area of that tissue was compared to the total infarct area; Troponin-T staining in adjacent slides was used to identify this tissue as cardiac muscle.

### Statistical analysis

All data generated in the pig functional study were compared with either a paired t-test or a Student’s t-test. Data are means ± SEM. Significance was considered to be $p < 0.05$.

## Supplementary Material

Refer to Web version on PubMed Central for supplementary material.

## Acknowledgments

The authors thank the Animal Care Program (ACP) veterinary staff, particularly M. Hardee, A. Smith, J. Fujimoto, and K. Jenne (University of California, San Diego) for their understanding and expertise in the animal handling, Holter monitoring, euthanasia, and care. We also thank C. Luo for his assistance during the porcine procedures, G. J. Kolaja for his expertise in histological analysis, and P. Chamberlin for facilitating the porcine histological and Holter analysis. Additionally, we thank Biosense Webster for providing the NOGA mapping technology. **Funding**: This work was supported by the Wallace H. Coulter Foundation (Miami, Florida), the National Science Foundation (101442) and the National Institutes of Health (1R43HL108459-01A1, 1R01HL113468-01A1). S.B.S.-N. held a graduate research fellowship from the National Science Foundation.

## References and Notes

1. Roger VL, et al. Heart disease and stroke statistics--2012 update: a report from the American Heart Association. Circulation. 2012 Jan 3.125:e2. [PubMed: 22179539]
2. Christman KL, Lee RJ. Biomaterials for the treatment of myocardial infarction. J Am Coll Cardiol. 2006 Sep 5.48:907. [PubMed: 16949479]
3. Rane AA, Christman KL. Biomaterials for the treatment of myocardial infarction a 5-year update. Journal of the American College of Cardiology. 2011 Dec 13.58:2615. [PubMed: 22152947]
4. Nelson DM, Ma Z, Fujimoto KL, Hashizume R, Wagner WR. Intra-myocardial biomaterial injection therapy in the treatment of heart failure: Materials, outcomes and challenges. Acta Biomater. 2011 Jan.7:1. [PubMed: 20619368]
5. Johnson TD, Christman KL. Injectable hydrogel therapies and their delivery strategies for treating myocardial infarction. Expert opinion on drug delivery. 2012 Nov 9.
6. Christman KL. Treating the leading killer. Sci Transl Med. 2012 Aug 8.4:146fs26.
7. Singelyn JM, et al. Naturally derived myocardial matrix as an injectable scaffold for cardiac tissue engineering. Biomaterials. 2009 Oct 1.30:5409. [PubMed: 19608268]
8. Singelyn JM, et al. Catheter-Deliverable Hydrogel Derived From Decellularized Ventricular Extracellular Matrix Increases Endogenous Cardiomyocytes and Preserves Cardiac Function Post-Myocardial Infarction. Journal of the American College of Cardiology. 2012 Feb 21.59:751. [PubMed: 22340268]
9. DeQuach JA, et al. Injectable skeletal muscle matrix hydrogel promotes neovascularization and muscle cell infiltration in a hindlimb ischemia model. Eur Cell Mater. 2012; 23:400. [PubMed: 22665162]
10. Valentin JE, Badylak JS, McCabe GP, Badylak SF. Extracellular matrix bioscaffolds for orthopaedic applications. A comparative histologic study. J Bone Joint Surg Am. 2006 Dec. 88:2673. [PubMed: 17142418]
11. Reing JE, et al. Degradation products of extracellular matrix affect cell migration and proliferation. Tissue Eng Part A. 2009 Mar.15:605. [PubMed: 18652541]
12. Daly KA, et al. Effect of the alphaGal epitope on the response to small intestinal submucosa extracellular matrix in a nonhuman primate model. Tissue Eng Part A. 2009 Dec.15:3877. [PubMed: 19563260]
13. Okada M, et al. Differential efficacy of gels derived from small intestinal submucosa as an injectable biomaterial for myocardial infarct repair. Biomaterials. 2010 Oct.31:7678. [PubMed: 20674011]
14. Seif-Naraghi SB, Horn D, Schup-Magoffin PA, Christman KL. Injectable extracellular matrix derived hydrogel provides a platform for enhanced retention and delivery of a heparin-binding growth factor. Acta Biomater. 2012 Jun 28.
15. DeQuach JA, et al. Simple and high yielding method for preparing tissue specific extracellular matrix coatings for cell culture. PLoS One. 2010; 5:e13039. [PubMed: 20885963]

16. French KM, et al. A naturally derived cardiac extracellular matrix enhances cardiac progenitor cell behavior in vitro. Acta Biomater. 2012 Dec.8:4357. [PubMed: 22842035]
17. Kubo H, et al. Increased cardiac myocyte progenitors in failing human hearts. Circulation. 2008 Aug 5.118:649. [PubMed: 18645055]
18. Lin YD, et al. Instructive nanofiber scaffolds with VEGF create a microenvironment for arteriogenesis and cardiac repair. Science Translational Medicine. 2012; 4:146ra109.
19. Leor J, et al. Intracoronary injection of in situ forming alginate hydrogel reverses left ventricular remodeling after myocardial infarction in Swine. J Am Coll Cardiol. 2009 Sep 8.54:1014. [PubMed: 19729119]
20. Laham RJ, et al. Intracoronary and intravenous administration of basic fibroblast growth factor: myocardial and tissue distribution. Drug Metab Dispos. 1999 Jul.27:821. [PubMed: 10383927]
21. Laham RJ, et al. Intracoronary basic fibroblast growth factor (FGF-2) in patients with severe ischemic heart disease: results of a phase I open-label dose escalation study. J Am Coll Cardiol. 2000 Dec.36:2132. [PubMed: 11127452]
22. Krause K, et al. Percutaneous intramyocardial stem cell injection in patients with acute myocardial infarction: first-in-man study. Heart. 2009 Jul.95:1145. [PubMed: 19336430]
23. Szummer KE, et al. Heart failure on admission and the risk of stroke following acute myocardial infarction: the VALIANT registry. Eur Heart J. 2005 Oct.26:2114. [PubMed: 15972293]
24. Velazquez EJ, et al. VALsartan In Acute myocardial iNfarcTion (VALIANT) trial: baseline characteristics in context. Eur J Heart Fail. 2003 Aug.5:537. [PubMed: 12921816]
25. Mukherjee R, et al. Targeted myocardial microinjections of a biocomposite material reduces infarct expansion in pigs. Ann Thorac Surg. 2008 Oct.86:1268. [PubMed: 18805174]
26. Ifkovits JL, et al. Injectable hydrogel properties influence infarct expansion and extent of post-infarction left ventricular remodeling in an ovine model. Proc Natl Acad Sci U S A. 2010 Jun 22.107:11507. [PubMed: 20534527]
27. Lin YD, et al. Intramyocardial peptide nanofiber injection improves postinfarction ventricular remodeling and efficacy of bone marrow cell therapy in pigs. Circulation. 2010 Sep 14.122:S132. [PubMed: 20837904]
28. Brown BN, Valentin JE, Stewart-Akers AM, McCabe GP, Badylak SF. Macrophage phenotype and remodeling outcomes in response to biologic scaffolds with and without a cellular component. Biomaterials. 2009 Mar.30:1482. [PubMed: 19121538]
29. Badylak SF, Freytes DO, Gilbert TW. Extracellular matrix as a biological scaffold material: Structure and function. Acta Biomater. 2009 Jan.5:1. [PubMed: 18938117]
30. Fujimoto KL, et al. Synthesis, characterization and therapeutic efficacy of a biodegradable, thermoresponsive hydrogel designed for application in chronic infarcted myocardium. Biomaterials. 2009 Sep 1.30:4357. [PubMed: 19487021]
31. Dib N, et al. Safety and feasibility of percutaneous autologous skeletal myoblast transplantation in the coil-infarcted swine myocardium. J Pharmacol Toxicol Methods. 2006 Jul-Aug;54:71. [PubMed: 16458541]
32. Hamamoto H, et al. Allogeneic mesenchymal precursor cell therapy to limit remodeling after myocardial infarction: the effect of cell dosage. Ann Thorac Surg. 2009 Mar.87:794. [PubMed: 19231391]
33. White HD, et al. Left ventricular end-systolic volume as the major determinant of survival after recovery from myocardial infarction. Circulation. 1987 Jul.76:44. [PubMed: 3594774]
34. McManus DD, et al. Prognostic value of left ventricular end-systolic volume index as a predictor of heart failure hospitalization in stable coronary artery disease: data from the Heart and Soul Study. J Am Soc Echocardiogr. 2009 Feb.22:190. [PubMed: 19084372]
35. Dib N, et al. A percutaneous swine model of myocardial infarction. J Pharmacol Toxicol Methods. 2006 May-Jun;53:256. [PubMed: 16460969]
36. Gyongyosi M, Dib N. Diagnostic and prognostic value of 3D NOGA mapping in ischemic heart disease. Nat Rev Cardiol. 2011 Jul.8:393. [PubMed: 21587214]
37. Christman KL, et al. Injectable fibrin scaffold improves cell transplant survival, reduces infarct expansion, and induces neovasculature formation in ischemic myocardium. J Am Coll Cardiol. 2004 Aug 4.44:654. [PubMed: 15358036]

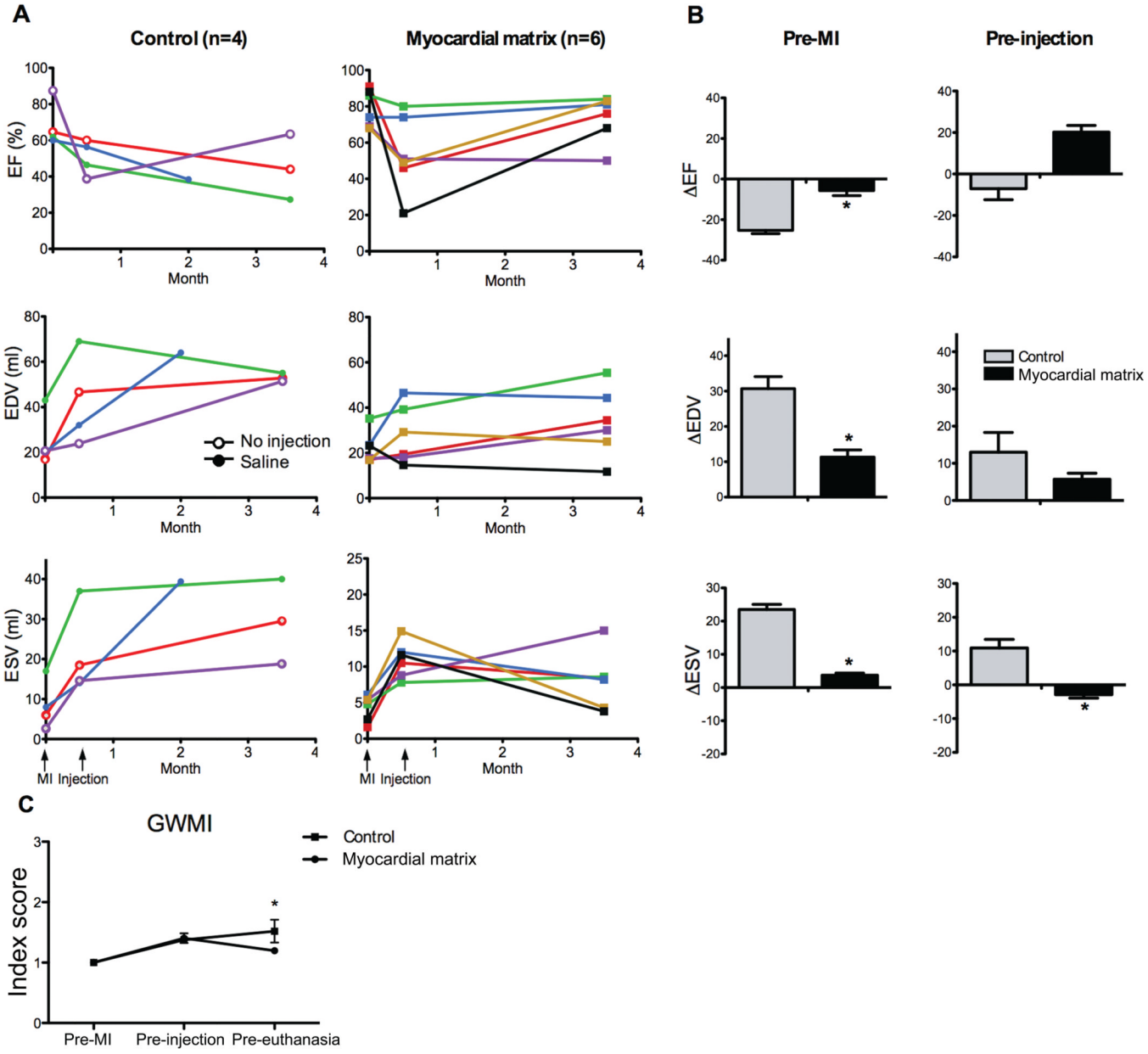


**Fig. 1.**

Echocardiographic data shows improvement after injection of myocardial matrix. (A) Ejection fraction (EF), end-diastolic volume (EDV), and end-systolic volume (ESV) are shown for each animal pre-MI, pre-injection (2 weeks post-MI), and pre-euthanasia for both the control ($n$ = 4) and matrix-injected ($n$ = 6) groups. Control animals that received saline injections are indicated with open circles (green and blue lines); animals that received no injection are represented with open triangles (red and purple lines). (B) Comparison of the absolute changes in EF, EDV, and ESV from either pre-MI baseline or pre-injection to the time of euthanasia. (C) Global wall motion index improves in matrix-treated animals. Note that error bars are present but not visible for the matrix-injected group at pre-euthanasia. All data are means +/− SEM. *p < 0.05 versus control (Student's t-test).

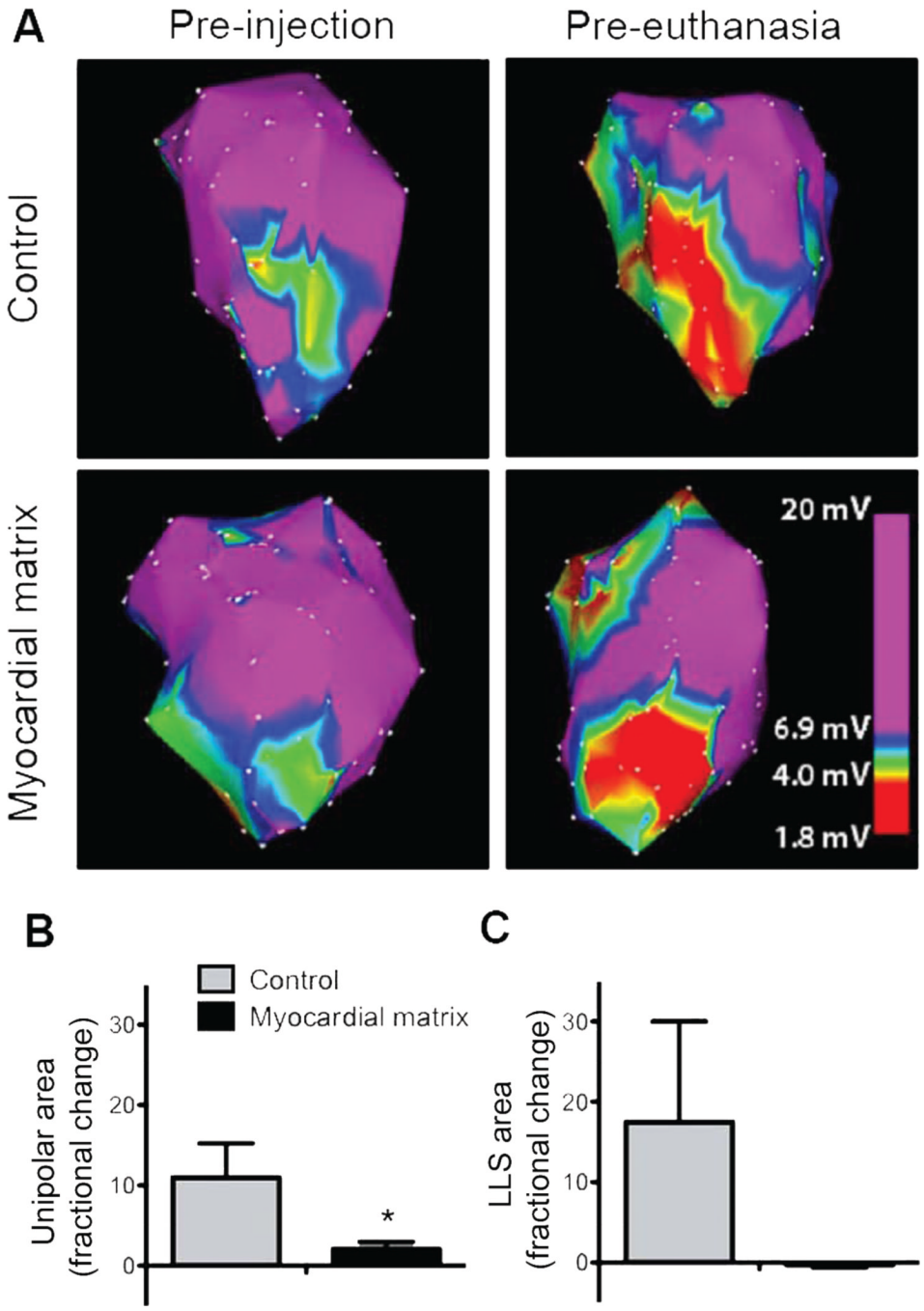


**Fig. 2.**

NOGA mapping and infarct expansion. (A) Representative unipolar area NOGA maps taken at time of injection and euthanasia. Images are thresholded to show the cutoff (6.9 mV) for the infarct area. (B) Infarct expansion calculated by unipolar area in myocardial matrix treated animals ($n = 6$) compared to the control group ($n = 2$). (C) Infarct expansion calculated via linear local shortening. Data are means +/− SEM. *$p < 0.05$ (Student's t-test).

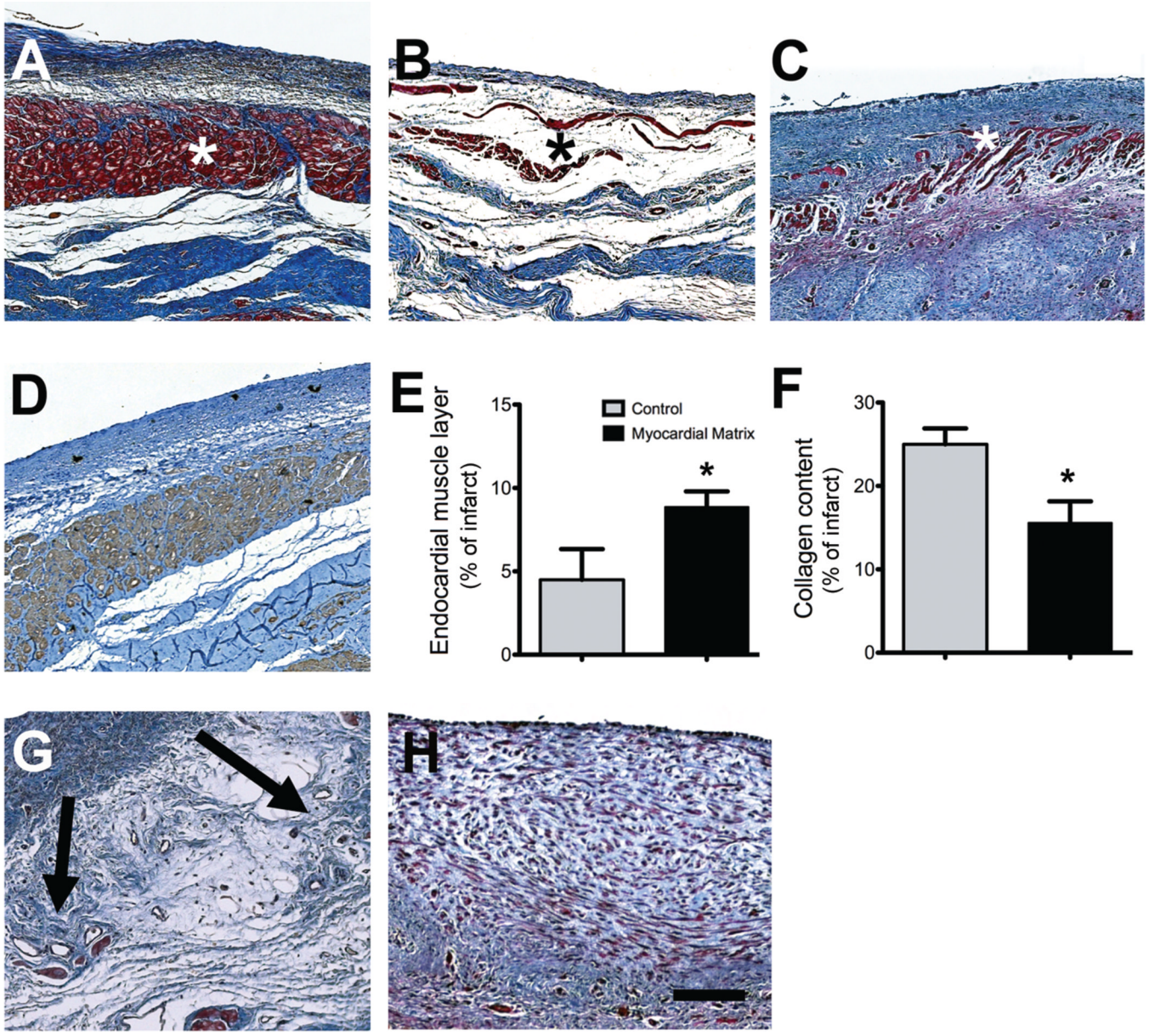


**Fig. 3.**

Histological characterization of infarcted pig hearts. (A to C) Masson's trichrome staining images are representative of 6 matrix-injected pigs and 4 control animals. (A) Matrix-injected hearts had a distinct, thick endocardium (red, indicated with an asterisk). (B) Non-injected control animals had a loose fibrillar layer (blue) beneath the endothelium. (C) In saline-injected control animals, the endocardium was moderately thickened (red) (D) An adjacent tissue section for the matrix-injected animal in (A) stained for cardiac troponin-T, indicating the presence of cardiomyocytes. (E) Area of endocardial layer of muscle as a proportion of the infarct. (F) Percentage of collagen content in the infarcts. Data are means +/− SEM and were obtained from Masson's trichrome slides (A to C). *$p < 0.05$, (Student's t-test). (G and H) Matrix-injected hearts contained foci of neovascularization in the area below the endocardium (G, arrows) but none of the saline or non-injected control hearts showed these areas of neovascularization (H). Scale bar is 200 μm.

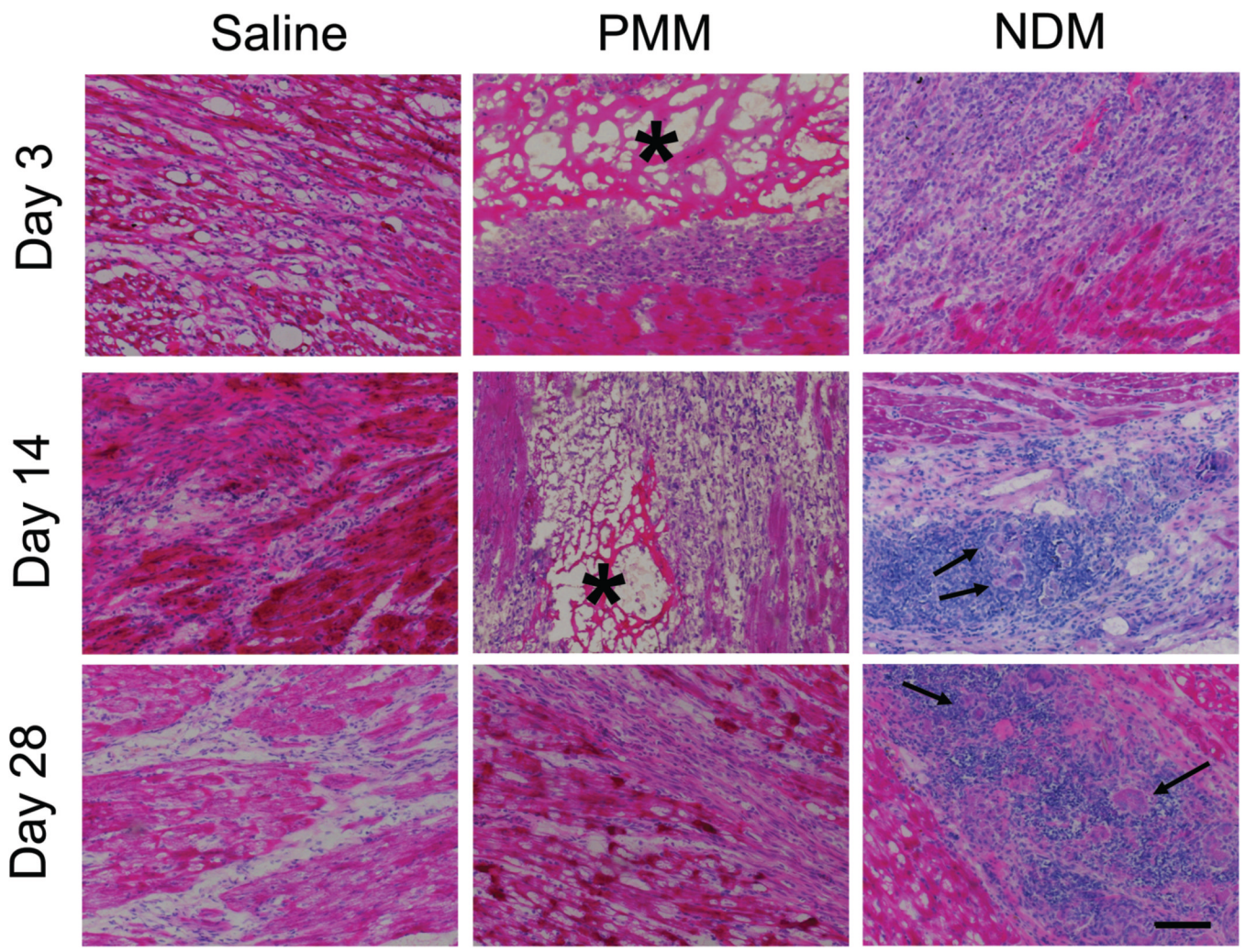


**Fig. 4.**

Cell infiltration in matrix-injected rat hearts. Representative histological sections from rat hearts injected with saline, porcine myocardial matrix (PMM), or non-decellularized matrix (NDM) at days 3, 14, and 28. Inflammation and multinucleated giant cells are present in the NDM groups at days 14 and 28 (arrows). The PMM (asterisk-marked porous network) was completely degraded by 28 days. Scale bar is 200 μm.

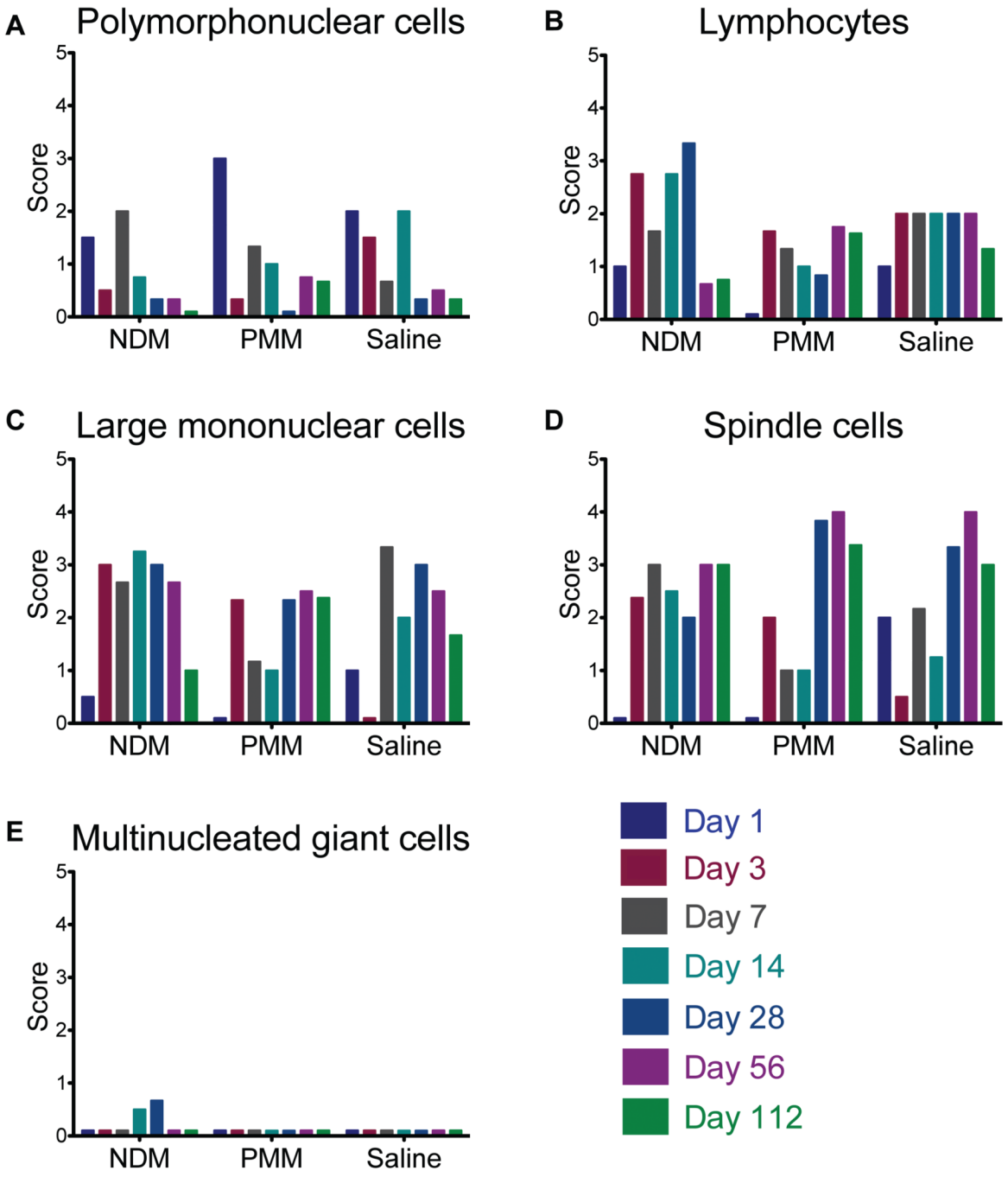


**Fig. 5.**

Matrix biocompatibility assessment in rats. (A to E) Average score for infiltration and degree of inflammation with respect to polymorphonuclear cells (A), mononuclear cells (B), lymphocytes (C), spindle cells (fibroblasts, myofibroblasts, and cardiomyocytes) (D), and multinucleated giant cells (E). On this scale, 0 = absent, 1 = minimal, 2 = mild, 3 = moderate, and 4 = marked. Due to freezing artifact, some tissue could not be analyzed and the data shown here is a composite score from 2 or 3 hearts per time point per group. .

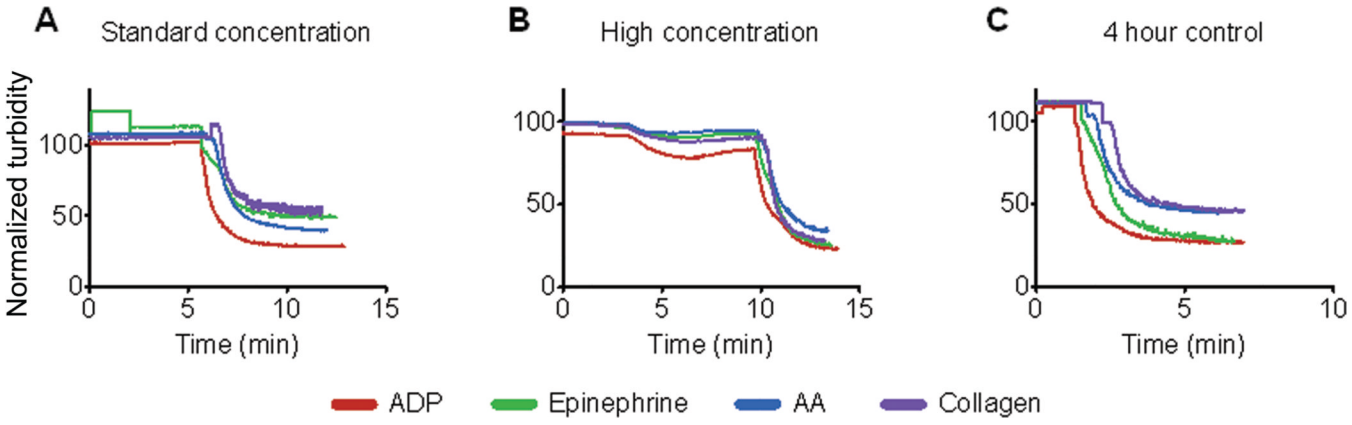


**Fig. 6.**

Platelet activation. (A and B) Addition of myocardial matrix to human platelet-richplasma was done at a standard concentration (1:10,000) (A) and a high concentration (1:2500) (B) and the samples were evaluated for at least five minutes. After the samples plateaued, agonists were added (at 10 minutes). (C) A control was performed after four hours to ensure normal activity of the samples and validity of the data in response to agonists. Data shown are representative traces from 4 repeated experiments.

**Table 1**

**Echocardiography data from porcine MI study**

Pre-injection measurements were taken 2 weeks after MI. Pre-euthanasia measurements were taken 3 months after injection, with the exception of one control, which died 2 months after injection. Data are means +/− SEM ($n$ = 4, control; $n$ = 6, myocardial matrix).

| | Control | | | Myocardial Matrix | | |
|---|---|---|---|---|---|---|
| **Echo measurement** | **Pre-MI** | **Pre-injection** | **Pre-euthanasia** | **Pre-MI** | **Pre-injection** | **Pre-euthanasia** |
| **EF (%)** | 68.5 ± 6.4 | 50.3 ± 4.8 | 43.3 ± 7.6† | 79.3 ± 4.2 | 53.5 ± 8.7 | 73.7 ± 5.3* |
| **ESV (mL)** | 8.4 ± 3.1 | 21 ± 5.4 | 31.9 ± 5.0† | 4.3 ± 0.7 | 10.9 ± 1.0 | 8.1 ± 1.6* |
| **EDV (mL)** | 25.2 ± 6.0 | 42.9 ± 9.9 | 55.8 ± 2.8‡ | 22.2 ± 2.9 | 27.8 ± 5.2 | 33.5 ± 6.2** |

*p<0.01,

**p<0.05 compared to control pre-euthanasia (student's t-test);

†p<0.01,

‡p<0.05 compared to pre-MI (paired t-test).

## Table 2
### Clotting times after exposure to myocardial matrix

The prothrombin time (PT) and the activated partial thromboplastin time (APTT) were obtained for human plasma samples after the addition of saline (control), the myocardial matrix at a standard concentration (1:10,000), and the myocardial matrix at a high concentration (1:2,500). Data are means +/− SEM ($n$ = 2).

| ECM:plasma | PT (s) | APTT (s) |
|---|---|---|
| Control (saline) | 11.65 ± 0.071 | 26.3 ± 0.0 |
| 1:10,000 | 11.75 ± 0.071 | 25.7 ± 0.141 |
| 1:2,500 | 11.75 ± 0.071 | 27.5 ± 0.566 |